United Technologies Research Center

TITLE:	Plasma-assisted Combustor Dynamics Control at Realistic Gas Turbine Conditions
TYPE OF REPORT:	Summary of Research
PRINCIPAL INVESTIGATOR:	Wookyung Kim
PERIOD:	03/16/2014 – 12/15/2015
INSTITUTION:	United Technologies Research Center 411 Silver Lane East Hartford, CT 06108
GRANT NUMBER:	NNX14AF53A
TECHNICAL CONTACT:	Dr. Wookyung Kim Phone: (860) 610-7266 Fax: 860-353-7921 Email: kimw@utrc.utc.com
BUSINESS CONTACT:	Mr. Shawn Gale Phone: (860) 610-7278 Fax: (860) 660-1130 Email: gales1@utrc.utc.com
DATE SUBMITTED:	3/7/2016

TABLE OF CONTENTS

1. Executive Summary

The central objective of this study is to demonstrate the effectiveness of implementing a plasma discharge to improve combustor dynamics and flame stability. Specifically, a nano-second pulsed plasma discharge (NSPD) was applied to a premixed gaseous fuel/air dump combustor for mitigation of dynamic combustion instabilities with a minimal NO_X penalty. The first phase of the project was focused on investigating the mitigation at ambient pressure and temperature while the second phase was dedicated to studying it at realistic gas turbine conditions.

As a result of Phase I, up to ~ 25 dB noise reduction from the methane/air dump combustor was observed in the presence of the NSPD. High speed imaging suggests that the NSPD relocated the flame stabilization point from the outer recirculation zone to the center zone. Due to the highly non-equilibrium temperature characteristic of the NSPD, the incremental increase of emissions in the presence of the discharge was minimal, typically around 0.5 $EINO_X$, while the increase of combustion efficiency could be significant and on the order of ~ 10 %. A new control algorithm that measured pressure oscillation amplitude, and actuated with plasma power was developed. This algorithm does not require knowledge/measurement of pressure oscillation phase, and therefore, avoids challenges associated with convective and actuator phase delays. The impact of NSPD on swirl-stabilized flames was also investigated for swirl numbers from 0 – 0.33. It is shown that the relative effect of NSPD for dynamics reduction decreases with increasing swirl due to the inherent decrease in nascent flame dynamics. All observations in the ambient condition suggest that the flame shape plays a central role in determining the degree of plasma effectiveness and that any noisy, outer recirculation zone stabilized flames will be significantly improved by this implementation of NSPD.

For the second phase, ~ 70 – 90 m/s flow velocity, ~ 580 K combustor inlet temperature, and ~ 5 atm in-combustor pressure were selected as baseline conditions to simulate a typical low-power environment of future aero engines. Also, some parametric surveys of varying velocity, temperature and pressure were carried out. As for the burner geometry and fuel, a similar dump combustor with fully premixed, low carbon chain fuels (methane and propane) was utilized to eliminate the higher order effects due to an incomplete mixing and the complexity of multi-phase flow at realistic gas turbine conditions. Similar to the Phase I, a significant reduction of combustor dynamics was observed, by two to four folds over a wide range of velocity (70 to 110 m/s) at the baseline temperature and pressure, and also at higher pressure (~ 7 atm). The plasma power required for the reduction increased linearly with increasing velocity, which implies that plasma power deposition per unit mass of flow is the key parameter for controlling combustor dynamics. The change of fuel from methane to propane clearly showed that propane requires significantly (2X) higher plasma power to achieve a similar level of noise reduction.

It was also observed that the lean blowout (LBO) limit at the low power gas turbine condition was significantly extended in the presence of the plasma, however, the substantial incomplete combustion occurs in the extended regime. Furthermore, it is shown that the LBO extension became increasingly more difficult to achieve with increasing pressure and decreasing plasma power. NO_X production was measured with two different velocities, temperatures and pressures, respectively. The results showed that incremental NOX production due to the presence of the plasma is low (~ < 1$EINO_X$) in general. The production was, however, increased with decreasing velocity and pressure, and increasing temperature.

This study shows that the plasma assisted combustor dynamics control is promising at realistic low-power gas turbine conditions as well as ambient condition without adding significant harmful emissions. We believe that future studies in the realistic gas turbine injector with realistic jet fuel are now appropriate to advance the TRL of this technology.

2. Introduction

Nano-second pulsed plasma discharge (NSPD) has gained increasing attention during the last two decades because of its outstanding capability to enhance various combustion phenomena. For example, the lean blowout limit extension and reduction of ignition delay time in premixed environments [1 – 3], and the stability-limit extension of diffusion flames [4] have been successfully demonstrated. The conceptual benefit and potential application of each of the enhancements include ultra-lean combustion which enables lower NOX aero-engine, faster ignition which makes high-efficiency supersonic combustion more viable [5], and more reliable diffusion combustion in higher speed coflow/crossflow which can be used for augmenting military aero-engines.

While previous studies have successfully demonstrated static flame stability improvements, the possible enhancement of dynamic flame stability in the presence of NSPD has been rarely studied until recently. Lacoste et al. [6] showed that mildly excited (~ 300 Pa) pressure oscillations can be significantly reduced with a passive control using the NSPD. They applied a phase-based control scheme to attenuate or aggravate pressure oscillations by a factor of two by changing actuation phase.

Despite the relatively short history of plasma assisted combustor dynamics control, the technology has far reaching impacts that include improved cabin comfort level, extended combustor life time, as well as a wider combustor operability range. This operability extension may aid the development of simplified, lighter weight and better-performing combustors with reduced staging requirements over a larger turndown ratio. Also, the improvements may facilitate a smoother transition from Rich-Quench-Lean combustors to the advanced Lean-Direct-Injection technologies.

Traditionally, both passive and active means for mitigating the pressure oscillation have been investigated. Passive methods include Helmholtz resonator [7], liner and baffles [8], fuel staging and piloting [9] and time delay manipulation [10] whereas active methods typically focus on fuel modulation [11]. While the applicability of these techniques has been successfully demonstrated for specific applications, many suffer from inherent drawbacks which include lack of robustness (passive), high system dependence (passive), intrinsic time delays (active), and significantly added complexity (passive and active). In contrast, application of NSPD in a lean premixed combustor can eliminate many of the drawbacks as it provides zero-time-delay active control with no moving parts or other complexity while also providing the relative benefits of low energy consumption, and low NOX production in comparison with other types of plasma.

Conceptually the NSPD alters key mechanisms of flame dynamics, specifically: fluctuation of flame speeds and ignition delay times, flame anchor point, fluid dynamic unsteadiness at the anchor point, flame sheet dynamics which include flame surface area variation and flame motion [12].

In more detail, the NSPD significantly accelerates key initiation/branching reactions of combustion [1] such that chemical time scales in the flame stabilization region become significantly shorter than fluid mechanic time scales. The segregation of the two time scales reduces the unsteady interaction between the combustion and fluid dynamics, resulting in augmented static flame stability, extension of the lean blowout limit and reduced liftoff height [13]. This reduced interaction also can decrease flamebase fluctuations in harsh fluid mechanic environments, and/or it can permit flame stabilization in a faster flow region with robustness to disruptive and unsteady fluid motion such as vortex shedding. The improved flamebase stability from NSPD, in turn, reduces the convection of these fluctuations and can ultimately affect the downstream flamesheet dynamics.

The current report consists of two parts: studies at i) ambient and ii) realistic gas turbine conditions. Three key questions are imposed in the first part;

- How much can the NSPD reduce thermo-acoustic oscillations?
- What is the underlying mechanism?
- How are emission and combustion efficiency characteristics altered?

For answering to those questions, the dynamics reduction in the presence of NSPD will be demonstrated for non-swirling conditions, over a range of equivalence ratio at ambient condition. Here, mechanisms that explain these reductions will be proposed. Also, the emission characteristics with the plasma discharge will be investigated. Next, a new plasma power-based control strategy is introduced. Lastly, the results are extended to swirling flow conditions that are more representative of practical combustor architectures. The second part will be focused on investigating the improvement of dynamic and static flame stabilities at elevated velocity, temperature and pressure conditions to confirm that this novel concept can be applicable to real gas turbines.

3. Experimental details

A photograph of the premixed dump combustor used in the ambient study is presented in Fig. 1a. The combustor consists of a 12.7 mm OD straight tube through which premixed room temperature methane/air is supplied by a variable swirl vortex valve, and a 45 mm OD circular dump volume confined by a ~ 915 mm long open-ended quartz tube. The vortex valve depicted in the sub-picture of Fig. 1a alters swirl strength by varying the split ratio between tangential and radial inlets. The typical chemical power generated by the ambient combustor was ~ 6 kW. Inlet bulk velocity was fixed at ~ 25 m/s.

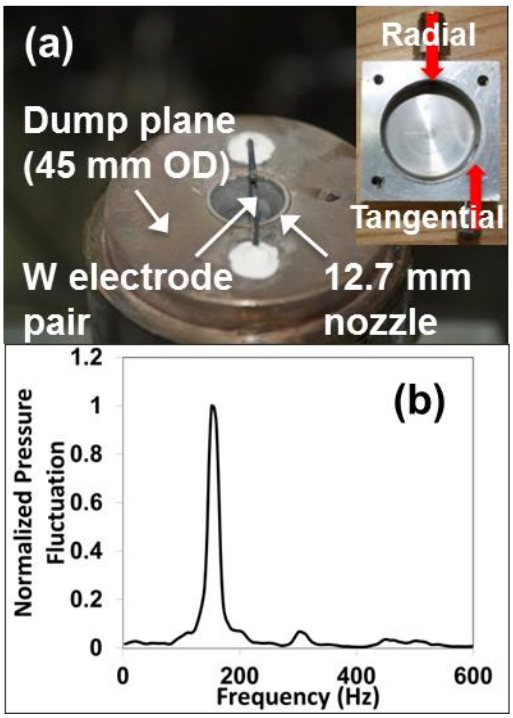

Fig. 1 (a) Photographs of dump combustor and vortex valve (top right); (b) typical uncontrolled pressure oscillation spectrum from the combustor

Blunted thoriated tungsten electrodes were mounted ~ 3 mm downstream from the dump plane with ~ 1.2 mm gap, and were connected with the NSPD generator. The typical operating conditions of the generator were ~ 7.5 kV p-p voltage, 15 – 30 kHz repetition rate (RR), and 15 ns pulse width. The NSPD RR was externally triggered by a delay generator.

Instrumentation included a probe microphone flush-mounted to the dump plane of the burner, pressure signal analyzer, a high speed voltage probe and a Rogowski coil, a spectrometer, a high speed camera, and gas emission sampling equipment for NO_X, CO, CO_2, O_2 measurements. Sampling was conducted using a single tip water cooled probe and the sampling location was ~ 230 mm above the dump plane on the centerline of the quartz tube.

A typical (normalized) pressure fluctuation spectrum is presented in Fig. 1b and was obtained without the NSPD at an equivalence ratio (ϕ) of 0.95 without swirl. Distinct high magnitude peaks were observed in the vicinity of 150

Hz and at its second harmonic, as well as broadband noise from ~ 430 – 530 Hz region. Absolute peak pressure fluctuation levels were ~ O(10^4) Pa, which are consistent with realistic pressure fluctuation levels and frequency profiles of aero-engine combustors. More detailed spectra and their interpretations will be shown in the result section.

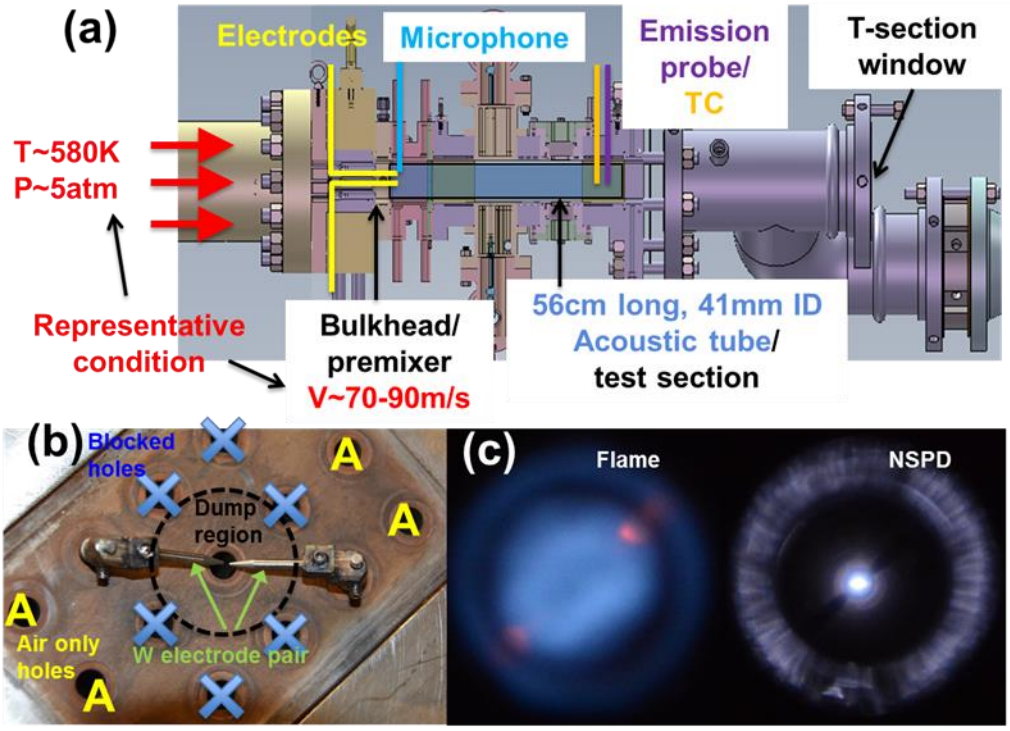

Fig. 2 (a) Schematic of high pressure and temperature rig which encloses the dump combustor; (b) Aft-looking-forward view of bulkhead. The dotted circle represents the location where the acoustic tube is placed at. (c) Aft-looking-forward view of flame (left) and NSPD (right)

Figures 2a and 2b shows a schematic of high pressure/temperature rig which encloses the dump combustor used in the elevated P/T test, and the aft-looking-forward view of the dump region, respectively. The most representative inlet condition was ~ 580 K T_3, ~ 5 atm P_3, and ~ 70 – 90 m/s V_3, where the T_3 and P_3 represent the temperature and pressure of combustor upstream, respectively, and the V_3 denotes the bulk velocity along injection nozzle. This combustor essentially mimicked the ambient design, but some dimensional modifications were required due to the spatial restriction of installation and availability of existing hardware. As a result, the OD of fuel injection tube and the length of acoustic tube were reduced to ~ 10.2 mm and 56 cm, respectively. Only one fuel injection tube located at the center was utilized for the experiment as shown in Fig. 2b. Other surrounding tube holes were either blocked or used as cooling air passages. No swirling flow was created in this configuration. Propane was used as a fuel in some cases of these high P/T experiments. Propane was chosen because it is a good candidate for simulating realistic gas turbine fuel chemistry, and still has practical advantages of low chain carbon fuels. The typical chemical power generated by the combustor was ~ 20 kW.

The aft-looking-forward view of flame (blue chemiluminescence on the left), electrodes (red glow on the left) and NSPD (bright spot on the right) of the high P/T rig are provided in Fig. 2c. The electrode configuration was similar with that of the ambient test, but the typical plasma p-p voltage and RR were

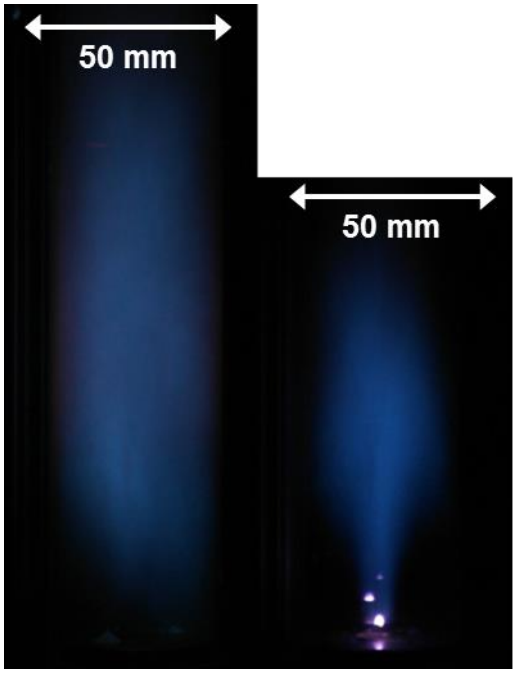

Fig. 3 Flame chemiluminescence images in the absence (left) and presence (right) of the 7.5 kV p-p, 25 kHz RR, NSPD (ϕ=0.9, SN=0)

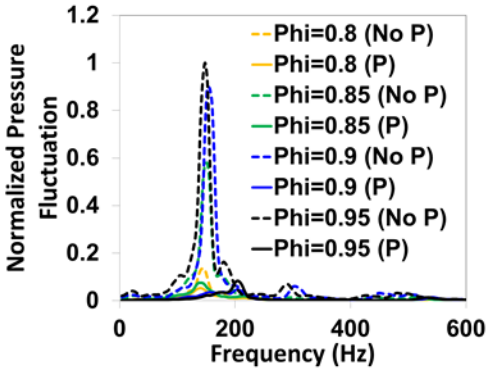

Fig. 4 Reduction of noise level in the absence (dashed) and presence (solid) of the NSPD. The discharge and flame conditions are identical with those of Fig. 2

increased to ~ 15 kV and up to ~ 100 kHz, respectively, to handle the elevated pressure. Instrumentation was also largely identical with the ambient test with the exceptions of probe microphone and emission sampling locations, 3 mm and 55 cm downstream of the dump plane, respectively.

The results from ambient configuration will be described first in the next section followed by those from the elevated P/T conditions.

4. Results

4.1 Investigation at ambient condition

A. Dynamics reduction

Time-averaged images of flame emission without (left) and with (right) the NSPD for ϕ = 0.9 and no swirl are presented in Fig. 3. Without the NSPD, the visual length of the flame in this ambient condition is ~ 150 mm and the flamebase appears to be stabilized at the outer recirculation zone (ORZ) of the dump plane and is vigorously fluctuating. In the presence of the NSPD, however, the flame was securely anchored to the center zone (CZ), where the NSPD was located, with minimal visible fluctuations. The flame length was also significantly shorter (~ 90 mm) and the observed noise level was dramatically reduced

As a quantification of the sound noise level difference in the presence/absence of the NSPD, the normalized pressure fluctuation spectra with varying equivalence ratio in the absence (dashed) and presence (solid) of NSPD are shown in Fig. 4. The NSPD conditions were identical with those of the previous figure. For all cases investigated in the ambient condition, consistently dramatic reduction of dynamics was observed in the presence of the NSPD. For example, the ϕ = 0.95 case showed ~ 25 dB reduction at the peak as well as the elimination of the second harmonic and the broadband noise near the 300 Hz and the 430 – 530 Hz region. It is noteworthy that the shift of the peak from the ~ 150 Hz (no NSPD) to the ~ 200 Hz (with NSPD) indicates a significant increase of the burned gas temperature, by ~ 15 %, with the plasma. The increase is not due to the plasma power addition, which was estimated as ~ 0.5 % of chemical power, but primarily due to a similar level of combustion efficiency improvement and the associated temperature increase. Comparable trend-wise reductions of pressure oscillations were observed for the lower ϕ cases even though the ratio of reduction

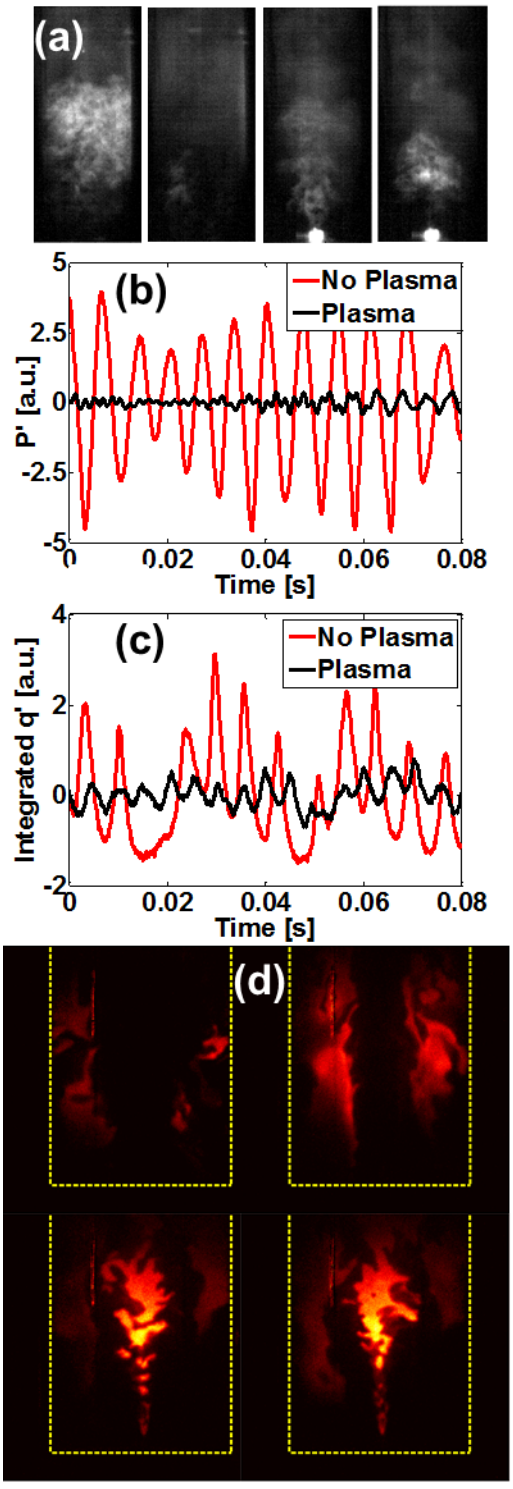

between cases with and without NSPD decreased with decreasing ϕ. As shown in the Fig. 4, this ratio of reduction was not caused by the loss of plasma control effectiveness, but by the inherently lower noise of the uncontrolled system for lower equivalence ratios. It is interesting to note that the spectral peak location without NSPD exhibits minimal sensitivity with decreasing ϕ which implies that nominal combustor temperature was not significantly altered. This is primarily attributed to the counteracting effects of decreasing ϕ and the increasing combustion efficiency associated with decreasing pressure oscillations.

B. Dynamics reduction mechanism

Unfiltered flame chemiluminescence high speed images (10 kHz frame-rate) obtained in the absence (left two) and presence (right two) of the NSPD at opposite phase are presented in Fig. 5a. One can find that continuous extinction/re-ignition occurs at each phase without the NSPD while the flamebase and downstream burn more steadily in the presence of the discharge. Simultaneous quantitative time-series data of pressure (p') and spatially integrated flame chemiluminescence (q') fluctuations are presented in Figs. 5b and c with (black) and without (red) the NSPD. The significantly smaller amplitudes for both p' and q' observed with the NSPD indicate that the flame burns much steadier in the time domain likely by spatially decoupling the burning process from fluid unsteadiness such as vortex shedding. Flame locations represented by 10 Hz OH Planar Laser Induced Fluorescence (PLIF) images are also provided in Fig. 5d. The flame randomly fluctuates at the outer zone of combustor without NSPD (top two), but steadily anchored at a center region when NSPD is present (bottom two).

Based on these observations, the hypothesis for noise reduction mechanism with the NSPD is depicted in Fig. 6. The current dump combustor, with similarities to more complex gas turbine combustor geometries, is composed of two zones: a center-zone (CZ) which is relatively steady for

Fig. 5 (a) Unfiltered, 10 kHz frame-rate flame chemiluminescence images at opposite phase in the absence (left two) and presence (right two) of the NSPD, corresponding (b) pressure fluctuation, and (c) spatially averaged chemiluminescence fluctuation time-series; (d) 10 Hz OH PLIF images in the absence (top two) and presence (bottom two) of the NSPD. Yellow dotted lines represent the combustor boundaries.

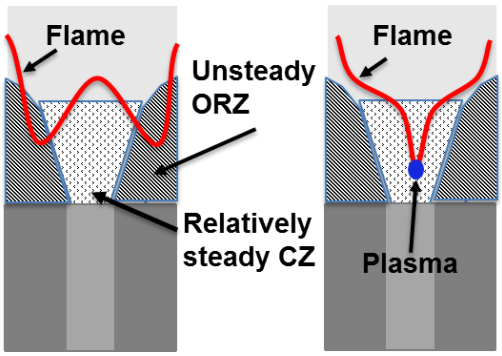

Fig. 6 Schematics of flame shapes without (left) and with (right) plasma

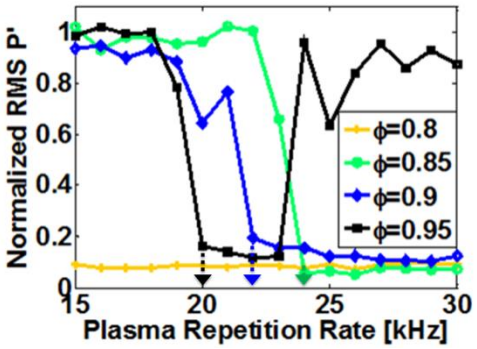

Fig. 7 Normalized p' as a function of plasma RR with varying ϕ

the conditions tested, and an outer recirculation zone (ORZ) that is highly affected by fluid unsteadiness. Without the NSPD, the flame is primarily stabilized in the ORZ. Fluid unsteadiness, coupled with combustor acoustics is amplified by the flame in a feedback loop that leads to limit-cycle oscillations with high unsteady pressures. The unsteady fluid mechanics in the ORZ are then exacerbated in this process and cause more unstable, less efficient combustion. In the presence of the NSPD, however, a flame is stabilized in the CZ where the fluid mechanics are steadier and more robust to fluid-acoustic coupling. Unlike previous efforts to control flame dynamics, the current NSPD application is essentially relocating the flame stabilization to break the link between the fluid mechanic fluctuation and flame oscillation.

For a validation of the proposed mechanism, we surveyed the normalized rms pressure fluctuations with varying ϕ as a function of plasma repetition rate (approximately proportional to plasma power) as shown in Fig. 7. Overall, no significant oscillation was detected at ϕ = 0.8 (yellow), therefore, applying NSPD showed no benefit. The visible flamebase location without the NSPD was ~ 100 mm downstream. With an increase of equivalence ratio to 0.85 (green), the flame was pulled upstream and started to reside near the ORZ. The flamebase fluctuation became visibly apparent without the NSPD, and the combustor became thermo-acoustically excited. When the NSPD was turned on and scanned to ~ 24 kHz RR, flame stabilized on the NSPD located at the CZ and sudden noise reduction was achieved. A similar propensity was observed for the ϕ = 0.9 case but its crossover RR was reduced to 22 kHz. At ϕ = 0.95, an interesting "bucket" shape was observed, i.e., the combustor was quiet only when the RR was between 20 kHz to 24 kHz. Outside of the bucket, the plasma power was either too weak (<20 kHz) to relocated the flame from the ORZ to the CZ, or excessively high (>24 kHz) such that the overly "energized" flame shifted upstream and started to reside/fluctuate in the ORZ. In all cases tested, the significant noise reduction was observed only when the flame was confined in the CZ, and any deviation from that shape aggravated the noise. These observations align well with our proposed mechanism depicted in Fig. 6, and further investigation about the combustor noise dependency on the flame shape will be discussed in Section 4.1E.

While the authority and mechanism of the NSPD for controlling the combustor dynamics were successfully demonstrated thus far, other important measures of combustor performance, NO_X production and combustion efficiency, will be the topic of the following section.

C. Emission and combustion efficiency

Figures 8a and b show incremental $EINO_X$, where $EINO_X$ is defined as grams of NO_X produced per kg fuel consumption, and combustion efficiency (η) calculated based on excess O_2 and CO production, in the presence of the NSPD with varying RR and applied voltage amplitude. Although it is clear that the NO_X

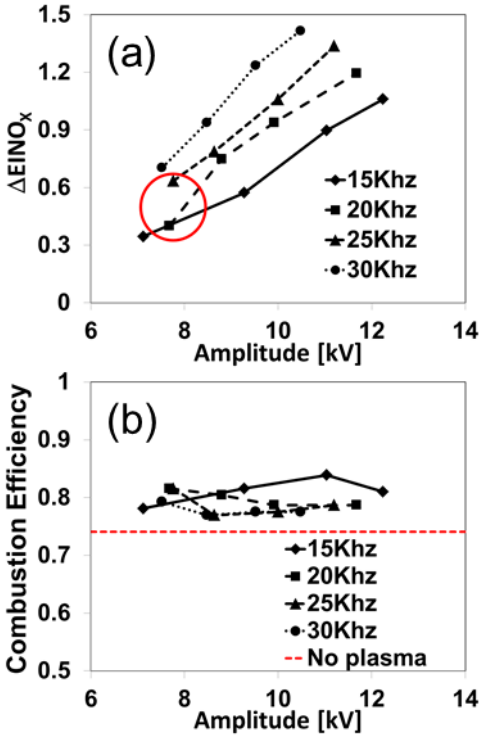

Fig. 8 (a) Incremental $EINO_X$ in the presence of NSPD; (b) Combustion efficiency with (black) and without (red) the NSPD

production is a linearly increasing function with the applied voltage and plasma RR, the $EINO_X$ increase was minimal and around ~ 0.5 EI for the typical range of NSPD used in the current ambient study (red circle). The incremental NO_X is due to a combined effect of increasing temperature associated with increasing η and plasma induced NO_X. Surprisingly, the η was not a strong function of the RR and voltage, but its increase in comparison with no NSPD case was consistently significant (~ 10%). This efficiency improvement represents ~ 17 times chemical power gain (~500 W) by investing a lower electrical power to generate NSPD (~ 30 W). According to a separate optical emission spectral analysis for the nitrogen second positive system, the time-averaged rotational temperature (equal to translational temperature at ambient pressure) was 1100 ± 50 K while the vibrational temperature was over 4500 ±100 K, which implies that the plasma is too cold to produce significant level of NO_X, but reactive enough to relocate a flame.

Thus far, we discussed that i) the combustor dynamics is a function of plasma RR or approximately plasma power, ii) produced NO_X increases linearly with the RR, and iii) η is a weak function of the RR. These three ideas are the basis of the newly proposed active control scheme, based on control of plasma power, shown in the following section.

D. Plasma power-based active control

Conventional phase-based dynamics control schemes utilize pressure/heat release fluctuation measurements from the combustor and an appropriately selected frequency to eliminate dynamics through destructive interference [6]. There are, however, intrinsic drawbacks of this method such as the inevitable actuator and convective delays that translate to complex spatial phase relations. These delays make complete control challenging. The power-based control proposed here does not require knowledge of the phase. Instead, the flame stabilization point is relocated to an appropriate region (CZ) to avoid thermo-acoustic coupling in the first place.

The control objective is to maintain a CZ stabilized flame with minimal power input to avoid high incremental NO_X production, while maintaining high η. The control algorithm was designed to find the crossover RR (pointed by arrows in Fig. 7) that represents a compromise between dynamics reduction and low NOx production. The same amount of noise reduction, ~25 dB shown in Fig. 4, was successfully demonstrated through this algorithm. While the details are not presented here, our Labview-based first generation controller continuously monitored rms pressure fluctuation level. Once a high pressure oscillation was detected, it started a rapid sweep in the plasma RR domain. The sweep stopped when the high gradient of the pressure oscillation was detected, and the system stayed in the RR until another high pressure oscillation was detected.

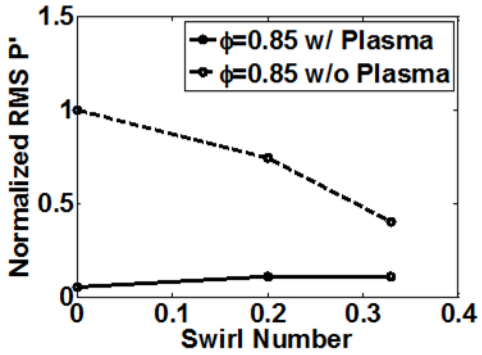

Fig. 9 Normalized rms pressure fluctuation with varying SN

Thus far, all investigations have been performed without swirl. In the next section, the change of plasma effectiveness under swirling flow will be briefly investigated.

E. Swirling flow and flame shape

The introduction of swirl is critical step in moving towards more realistic gas turbine combustor architectures and provides an easy way to change flame shape at fixed flow conditions. In this way, we can validate both the practicality of the current technique and our proposed mechanism, both of which are closely tied to flame shape.

Similar high speed imaging and corresponding p' and q' measurements, as in Fig. 5, were conducted at 0.33 swirl number (SN) in the absence/presence of the NSPD. The 0.33 SN, calculated from separate laser-doppler-velocimetry (LDV) measurements, was chosen because it was close to the maximum swirl number before flashback for the current flow conditions. The swirl numbers utilized in this study reside below the critical level for vortex breakdown [14]. Even without the NSPD, the visible flame length became shorter and the burning appeared steadier in comparison with no swirl case. It was still clear, however, that the flame assisted by the NSPD burned in much steadier manner.

As a quantification, Fig. 9 shows the normalized rms pressure fluctuation with varying swirl in the absence (dashed) and presence (solid) of the NSPD at $\phi = 0.85$. The flame became quieter with increasing swirl even without the NSPD. This decrease in pressure fluctuation is a result of the flame being stabilized near CZ with the increasing swirl, and due to the reduced size of ORZ. As a result, the incremental benefit of NSPD decreases, not as much because plasma loses its effectiveness (the controlled rms pressure does not change appreciably), but because the uncontrolled flame inherently becomes quieter. Although no systematic investigation has been attempted, we observed that even the swirl stabilized flame exhibited higher dynamics when perturbed (e.g., higher velocity) so its flame shape changed to ORZ stabilization. In that situation, the effectiveness of NSPD was more consistent with low swirl conditions, which implies that i) swirl is only one factor in determining flame shape which is a more intrinsic parameter for setting flame robustness to dynamics [15], and ii) the plasma stabilization effect observed in the current study should still hold for any ORZ stabilized flame shape.

In the following section, our findings in the ambient experiment will be generalized and aligned with future aeronautics challenges.

F. Implications of ambient tests

As discussed in the Introduction, the operability limit extension is one of the key requirements for developing simpler, light-weight future aero-engine combustors with improved performance. To quantify the operability limit extension in the ambient condition, Fig. 10 presents the static and dynamic flame stabilities quantified by combustion efficiency and pressure oscillation level, respectively. In the presence of the NSPD (red circle), the static flame stability is increased by ~ 10 % and, simultaneously, the dynamic flame stability is improved by ~ 10X in comparison to data without NSPD (empty diamond outside of the red circle).

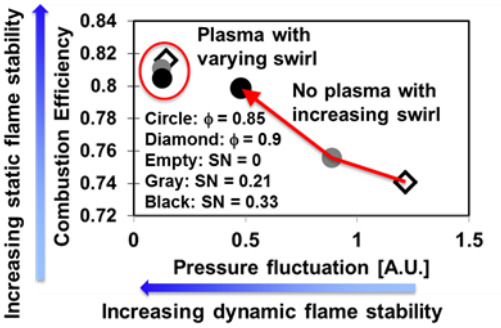

Fig. 10 Widened operability limit with the NSPD

From this observation, three major potential impacts are expected: a more device-independent solution for inherent flame dynamics, reduction of the combustor size, and enablement of potential for new combustor architectures. The improvements observed in Fig. 10 were achieved for generic combustor geometry/conditions and the versatility and robustness of the current concept may be equally applicable to other combustor geometries/conditions. The improved operability due to the augmented flame stabilities may lead to improved efficiency over a larger turndown ratio, and eventually may reduce staging requirements. The reduced fuel staging in turn results in a simpler (and smaller) low emission advanced combustor with lower associated cost and weight. In addition, Fig. 10 suggests that the improvement with NSPD is comparable if not better than the effect of increasing SN (grey and black dots outside of the red circle). This observation implies that the NSPD may completely augment or replace the role of swirl in the flame stabilization process.

Based on the promising results of the ambient configuration, the central objective of the following section is to investigate if the similar improvements can be achieved in the realistic gas turbine conditions.

4.2 Investigation at realistic gas turbine condition

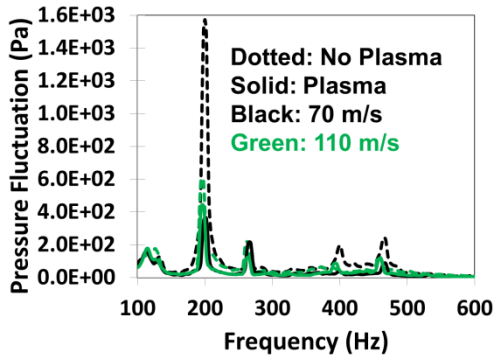

Fig. 11 Reduction of noise level in the absence (dashed) and presence (solid) of the NSPD. The discharge and flame conditions are 15 kV p-p, 80 kHz RR and 0.58 ϕ (propane), 580 K T_3, 5 atm P_3, respectively.

A. Dynamics reduction

Figure 11 shows the representative pressure fluctuation spectra in the high P/T rig in the absence (dotted) and presence (solid) of the NSPD at two different inlet velocities (V_3), 70 m/s (black) and 110 m/s (green). Inlet pressure (P_3) and temperature (T_3) are departed from ambient and elevated to 5 atm and 580 K, respectively. Carrying out experiments at this flow condition is important because it represents a typical ground idle (GI) regime of future aero-engine combustors where a majority of combustor dynamics occurs. Propane was used as a fuel for this particular example. The propane flame under the high P_3 and T_3 became essentially more stable than the methane flame in ambient condition. For example, the peak pressure fluctuation of 70 m/s case was significantly lower (~1600 Pa) than that of ambient methane flame (O(10^4) Pa) even without the involvement of NSPD. The peak level was further reduced to <400 Pa with the NSPD. It was confirmed by a phenomenological aft-looking-forward visualization that the flame anchor point was relocated from ORZ to CZ when the drastic noise reduction was achieved with the NSPD. This observation is well aligned with the previous discussions made in the ambient experiments.

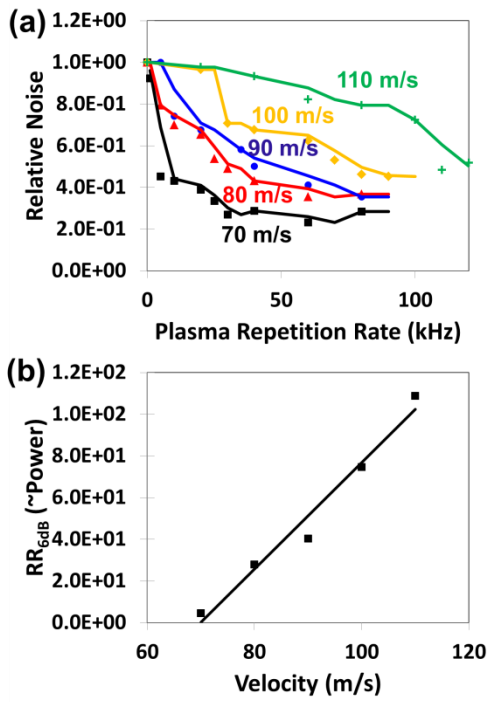

Fig. 12 (a) Relative noise (the ratio of peak pressure fluctuation in the presence of NSPD to the one in its absence) of methane flame at ϕ_{NLBO} with varying inlet velocities; (b) Required RR to achieve 6 dB (~ 50%) noise reductions as a function of inlet velocity. Plasma p-p voltage, T_3 and P_3 are identical with those of Fig. 11.

The degree of reduction, however, was lessened in the higher velocity condition as shown from the green curves where the reduction from ~ 600 Pa (no NSPD) to ~ 450 Pa (with NSPD) is represented. It is not clear whether the diminution of plasma effectiveness is caused by higher inlet velocity or already-low baseline (no NSPD) noise. Unfortunately, we couldn't find a set of conditions from the propane flame, which could isolate one of the two possibilities. On the contrary, we could find a set of ϕ's with methane flame, which produced a similar level of baseline noise over a wide range of inlet velocity at the equivalent P_3 and T_3. In particular, our methane flame typically generated identical level of baseline noise at "near" lean blowout equivalence ratio defined by $\phi_{NLBO} = \phi_{LBO} + 0.01$. As a result, all dynamics results in this study were obtained at the ϕ_{NLBO} with methane fuel unless stated otherwise.

The relative noise, defined by the ratio of peak pressure fluctuation in the presence of NSPD to the one in its absence, is plotted as a function of RR in Fig. 12a. The figure quantifies the effectiveness of plasma with varying V_3 under the identical baseline noise. The V_3 investigated varies from 70 m/s to 110 m/s such that it can survey most of low to mid power gas turbine inlet velocities. As shown from the figure, the relative noise monotonically increases with increasing V_3 for identical RR (or identical plasma power deposition). The same results are depicted in a different way in Fig. 12b, i.e., required RR to achieve 6 dB (50%) noise reductions as a function of V_3. The figure further shows that the required RR (or required plasma power) is a linearly increasing function with increasing V_3. We believe that the linear propensity implies that the plasma power deposition (per unit mass of medium for the varying inlet condition) can still be a key control parameter for the current system, which confirms the discussion in Section 4.1D.

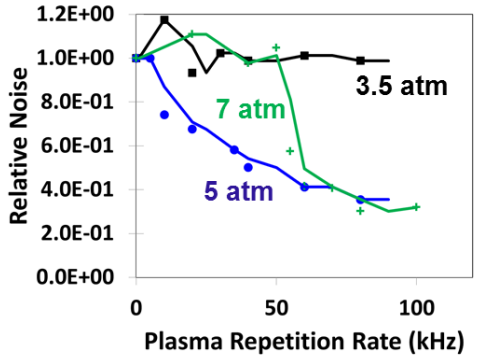

Fig. 13 Relative noise of methane flame at ϕ_{NLBO} with varying pressures. Plasma p-p voltage and T_3 are identical with those of Fig. 11 while V_3 is 90 m/s.

We also surveyed the effectiveness of plasma with varying P_3 as shown in Fig. 13 where the relative noise is plotted as a function of RR at three different P_3's, 3.5, 5, and 7 atm. The blue curve (5 atm P_3 at 580 K T_3 and 90 m/s V_3) is a re-plot from Fig. 12b, and it represents the usual monotonic decrease of noise with increasing plasma power starting from ~5 kHz RR. The 7 atm pressure case, on the contrary, shows a step-wise reduction: a minimal sign of noise reduction up to 50 kHz RR followed by a rapid reduction starting from 55 kHz. As a result, the RR for 6 dB reduction at the high pressure is ~ 60 kHz, or ~50% higher than that of the low pressure condition. The higher power requirement is

originated from two facts; plasma power deposition per unit mass of medium decreases with increasing pressure, and plasma discharge itself becomes weaker at the high pressure (or low reduced electric field) environment. While the former supports the previous hypothesis of specific plasma power deposition, it is noteworthy that the 7 atm is very close to a discharge breakdown limit for the currently applied voltage (~ 15 kV) and electrode configuration.

It may be noteworthy that the resulting relative noise after a complete control for those two pressures is almost identical as ~ 0.3 in spite of the power requirement difference. The similarity may be caused by the fact that our control objective is disruptively relocating a flame, not continuously changing noise amplitude by a phase control. In other words, the flame relocation is harder at higher pressure because of the reasons aforementioned; but the resulting dynamic stability of a combustor will be similar regardless of the pressure once flame is relocated and anchored at the CZ.

It is interesting that the relative noise at 3.5 atm shows minimal reduction in the presence of the NSPD. It is because the baseline noise level (in the absence of NSPD) at this pressure was already low as ~ 130 dB, which is essentially identical with the fully controlled noise level in the other two higher pressure conditions. As we discussed in Section 4.1E, the NSPD and current control scheme can reduce the noise level of a dynamically unstable combustor where, otherwise, flame is anchored at ORZ. However, they do not further improve the noise characteristic of an already stable combustor with a CZ anchored flame.

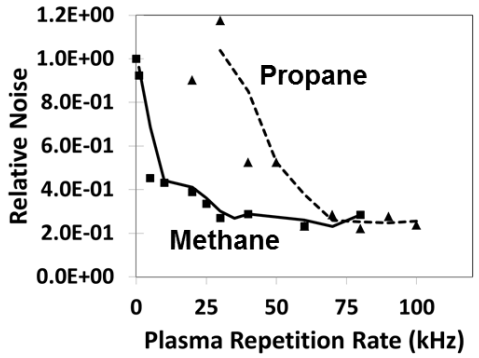

Fig. 14 Relative noise of methane (solid) and propane (dotted) flames at ϕ_{NLBO}. P_3, T_3, and V_3 are 5 atm, 580 K and 70 m/s, respectively, and plasma p-p voltage is 15 kV.

A brief comparison of plasma effectiveness for methane and propane fuels is provided in Fig. 14 as the last variation of dynamics study. One can find from the figure that the relative noise reductions observed from those two fuels show trend-wise similarity, but the propane requires significantly higher plasma power to attain the identical level of relative noise. The complete control of methane flame, for example, was reached at ~ 35 kHz RR while propane fuels required ~70 kHz RR. It is noteworthy that the ϕ_{NLBO} of the two tests were drastically different, 0.72 for methane, and 0.58 for propane. The baseline dynamics levels (in the absence of NSPD) of each fuel are significantly different as well, ~140 dB for methane and ~150 dB for propane. We do not have a solid answer to the questions which portion of the difference is caused by the discrepant initial conditions of each experiment, or what level of dissimilarity is originated by discrepant plasma chemistries in two different fuels. The answer should be addressed in future studies because the reasons of power requirement variation for different fuels will be a key element for expanding the current concept to realistic higher-carbon-number aero-engine fuels like Jet-A.

B. Static flame stability and emission

Static flame stability improvement, usually measured by lean blowout limit (LBO) extension, is one of the most significant firsthand benefits of the NSPD. While previous studies have successfully demonstrated the improvements [1 – 5], the majority of the investigations were for laboratory scale, ambient (or lower) pressure combustors.

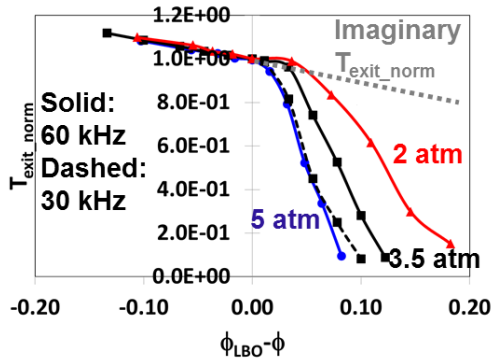

Fig. 15 Normalized combustor exit temperature in the reduced ϕ domain with varying pressure. The grey dotted is an imaginary line of complete combustion. Plasma p-p voltage, P_3, T_3, and V_3 are identical with those of Fig. 14.

Fig. 15 shows normalized (and reduced) combustor exit temperature (T_{exit_norm}) in the reduced ϕ (ϕ_r) domain at three elevated P_3's, 2 (red), 3.5 (black) and 5 atm (blue). It is to quantify the possible LBO extension at realistic gas turbine condition, T_3 and V_3 were kept fixed at 580 K and 70 m/s, respectively, and methane was the fuel. The T_{exit_norm} and ϕ_r are defined as follows, respectively,

$$T_{exit\_norm} = \frac{T - T_{No\_comb}}{T_{LBO} - T_{No\_comb}}$$

$$\phi_r = \phi_{LBO} - \phi$$

,where the T_{No_comb} and T_{LBO} represent the combustor exit temperatures without combustion, and just before the LBO, respectively. There was no NSPD involved for the negative ϕ_r (i.e. before LBO) because a flame was self-sustaining in that regime. The T_{exit_norm}'s of three pressures in the negative ϕ_r are collapsed to single curve and decreased linearly with increasing ϕ_r. The linear decrease implies that combustion efficiency (η) and the specific heat of mixture over the regime can be reasonably assumed as constants. It was confirmed, in fact, from a separate CO/UHC measurement that the calculated η over the regime was significantly high (>~99.9%), therefore approximately constant. One may imagine an extrapolation of the linearity to the positive regime of ϕ_r (i.e., after LBO) as the dotted grey curve depicts in the figure. The line would, then, represent an imaginary T_{exit_norm} if complete combustion occurred over the positive ϕ_r, from which a degree of incomplete combustion can be quantified by the deficiency.

The three curves depicted in the positive ϕ_r regime show a LBO extension due to the NSPD. While it is clear that the NSPD drastically improves the static flame stability (0.08 – 0.18 equivalence ratio), the improvement becomes more difficult to achieve with increasing pressure. Specifically, the improvement at 5 atm (~ 0.08 ϕ_r) is less than a half of the one at 2 atm (~ 0.18 ϕ_r). The degree of incomplete combustion, again deficiency from the grey curve, is also exacerbated with increasing pressure. The reduction of plasma power as well as the increasing pressure also significantly aggravates the LBO extension and η. The black dotted curve obtained with ~ 50 % plasma power deposition (30 kHz RR) shows that the LBO extension is reduced by 0.025 ϕ_r in comparison with the normal power deposition (60 kHz RR) at the same pressure. The corresponding η of 30 kHz RR is also diminished by ~ 20 – 30 %. The dependence of static flame stability enhancement on pressure and plasma power deposition may also indirectly confirm the central role of our control parameter, plasma power deposition per unit mass of medium.

The significant incomplete combustion observed above may not be the most promising results for real world state-of-the-art combustor applications. However, engineering solutions such as implementing spatially distributed NSPD's or depositing higher plasma power to enhance the η will help to mitigate or eliminate the problem. Also, expanding the area of applications to more one-time, *ignition* focused

applications, such as high altitude relight or a fast ignition of auxiliary power unit at rapid spool stage, will unburden the poor η performance observed.

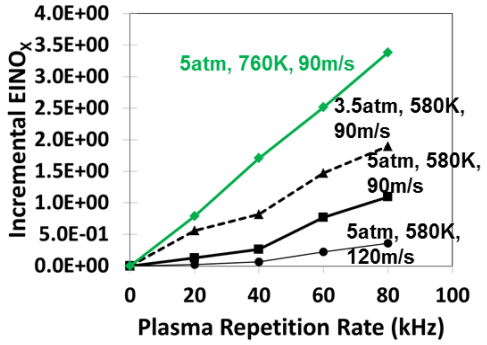

Fig. 16 Incremental $EINO_X$ at two different pressures, temperatures, and velocities. Plasma p-p voltage is 15 kV.

The other important static characteristic, NSPD-induced NO_X emission for a realistic methane/air premixture, is depicted in Fig. 16. The incremental $EINO_X$ at the representative inlet condition is not significantly higher than ~ 1$EINO_X$ even at the highest RR case as shown from the thick black solid line. It is noteworthy that the 1EI is not a significant value under the current and near-future NO_X regulations.

We chose two different conditions for each V_3, P_3 and T_3 for a brief investigation of the NO_X dependence on inlet conditions. The results show that the incremental $EINO_X$'s are linearly increasing with increasing RR for all conditions tested, but the slopes are strongly dependent on them. The linear dependency on plasma RR is not surprising even though detailed NO_X chemistry in the presence of NSPD is a topic not clearly understood thus far and beyond the scope of the current study. It is believed that there exist multiple major reactions closely associated with the NSPD induced NO_X production, for example, [16],

$$N_2^* + O_2 \rightarrow N_2 + O + O \text{ (dissociative quenching)}$$

$$N_2^* + O \rightarrow NO + N \text{ (reactive quenching)}$$

$$N + O_2 \rightarrow NO + O \text{ (2}^{nd}\text{ Zel'dovich)}$$

$$N + OH \rightarrow NO + H \text{ (3}^{rd}\text{ Zel'dovich)}$$

,where N_2^* is multiple excited electronic/vibrational states of N_2 generated due to the NSPD. The first reaction which induces "rapid atomic heating" is believed as one of the major production reactions of atomic oxygen along with the electron impact dissociation reaction between molecular oxygen and electrons [16, 17]. The atomic oxygen, then, reacts with the excited N_2 to produce NO as shown in the second reaction. NO can be further produced in afterglow stage by the third and fourth reactions. By varying the RR of NSPD, what one essentially does is directly altering frequency at which the top two reactions occur. Meanwhile, one can find that every NSPD pulse of the current study is discharged to a fresh portion of flow which did not previously experience plasma; i.e., states of medium the individual pulse experiences is refreshed to be identical. The statement can be confirmed from the fact that the product of RR time scale (> 10 μs) and flow velocity (~ 100 m/s) is longer than the discharge length scale (< 1 mm electrode tip sharpness). Therefore, the NO concentration ([NO]) produced by the set of chemical reactions above is independent among pulses and can be arithmetically added for each event of discharge. The linear propensity of [NO] to the RR represented in the figure is a result from the additive nature.

The [NO] is decreased with increasing V_3 as shown from the thick (90 m/s) and thin (120 m/s) solid black curves. The firsthand reason of decrease is again the decreasing plasma power deposition per the unit

mass of medium at the higher V_3. It is noteworthy, however, that the [NO] of the higher V_3 decreases more than two folds while its power deposition ratio is still as high as ~ 66 % of that of lower V_3. The additional decrease of [NO] is probably because electrode tips are maintained at a lower temperature with the high speed flow due to an enhanced heat transfer. The thermionic emission of electrons from the tips, which further produce N_2*, O, and therefore NO_X, is reduced under the low temperature environment.

The higher NO_X production at 3.5 atm (dotted black) in comparison with the 5 atm P_3 (thick solid black) is primarily due to the increase of power deposition ratio as well. It is also interesting, however, that the ratio increase at the lowered pressure is ~ 40 %, but the corresponding [NO] increase is higher as ~ 70 %. The further increase of NO should be partially attributed to the enhanced plasma intensity at the lower P_3 (or higher reduced electric field). The rate coefficients of the N_2* and rapid heating O atom production reactions are possibly pressure dependent as well.

The variation of inlet temperature from 580 K (black solid) to 760 K (green solid) alters [NO], approximately by three times. The drastic increase should be due to the combining effect of higher power deposition ratio, more significant thermionic emission at the higher temperature, and more intense discharge under the higher reduced electric field. This observation may raise a restriction against applying this technology to a high power condition. But it is noteworthy that combustor dynamics may become an issue more frequently at low power condition. Also, an electrode design including clever positioning with an active cooling will further reduce the tip temperature which must relieve NO_X production due to the thermionic emission.

As a final comment, it should be noted that there still exist challenges and unanswered questions for this technology to be applied in real gas turbines: namely, short electrode lifetime, significant electro-magnetic interference (EMI), and possibly increased difficulties with realistic injectors and fuel types. Single pair of tungsten electrodes in the elevated P/T study, for example, could not be used more than 5 – 6 hours of continuous run because of serious oxidation and erosion on the tip region. The EMI from the NSPD was intense because of high voltage ramp rate (~ 2 kV/ns) such that major instrumentations were failed multiple times. Partially premixed, partially vaporized Jet-A/Air stream from a realistic high shear injector can exacerbate the reliability of plasma discharge and flame ignition. Implementing durable electrodes such as ceramic coated copper alloy material, developing more universal EMI shielding methods, and better understanding the NSPD behavior in the wet environment, therefore, need to be further studied before this technology becomes appropriate to advance higher TRL.

5. Conclusions

The current study showed an effort to investigate a new means for mitigating combustor dynamics and also widening the operability range. The experiments were carried out in two configurations, ambient P/T at ~ 25 m/s inlet velocity, and realistic gas turbine P/T at a few fold higher inlet velocity.

For the ambient test, nano-second pulsed discharge (NSPD) was applied to a premixed methane/air dump combustor which typically produced ~ $O(10^4)$ Pa pressure fluctuations. With the NSPD, the flame length was shortened by ~ 40%, and the peak pressure fluctuation level was decreased by up to ~ 25 dB. A noise reduction mechanism was proposed by investigating flame shapes in the absence/presence of the NSPD. NSPD relocated the highly fluctuating, outer recirculation zone stabilized flame to more quiescent center zone. The noise reduction is essentially achieved by unlinking a fluid mechanical fluctuation from flamebase motion.

Incremental $EINO_X$ and combustion efficiency in the presence of NSPD were quantified as ~ 0.5EI, and ~ 10%, respectively, and the small added $EINO_X$ was attributed to high variation between the rotational and vibrational/electronic temperatures of the NSPD.

A plasma power-based control scheme, which employed the plasma repetition rate as the control parameter, was successfully demonstrated. Identifying crossover repetition rates was a control objective to balance combustor noise, NO_X production, and combustion efficiency.

Swirling flow was implemented to validate the practicality of the current technology and the proposed mechanism. Increased swirling flow resulted in shorter flames that burned more steadily even without the NSPD. Significant combustion dynamics improvement was observed for all SN conditions in the presence of the NSPD, however, the effectiveness of NSPD decreased with increasing swirl strength. Results suggest that flame shape, not absolute swirl number, is the key in determining the effectiveness of the NSPD.

Improved static and dynamic flame stabilities, and resulting operability limit extension in the presence of the NSPD were summarized. The NSPD stabilized combustor may have potential benefits in terms of versatility and simplicity, and furthermore it may shift a paradigm of combustor architecture.

From the elevated P/T experiments, a significant reduction of combustor dynamics (~ 6 – 12 dB) was observed over a wide range of inlet velocity (70 – 110 m/s). The power required for the reduction linearly increased with increasing velocity. Accordingly, plasma power deposition per unit mass of medium at the varying inlet condition was believed as the key control parameter. The behavior of noise reduction was different depending on pressure and type of fuel as well. Higher pressure (7 atm) required higher plasma power deposition for a complete control. The combustor already stable at a low pressure (3.5 atm) was not affected by the presence of NSPD. Propane required significantly higher plasma power (~ 2X) in comparison with methane until the combustor dynamics became completely controlled. The reason was not clearly understood in the current study.

Significant lean blowout limit extensions (0.08 – 0.18 equivalence ratio) were observed with varying inlet pressure. The extension, however, became more difficult to achieve with increasing pressure and decreasing plasma power because of the lowered plasma power deposition per unit mass of medium. Substantial incomplete combustion was also observed in the extended region.

Incremental NO_X production in the presence of NSPD was measured with two pressures, temperatures and inlet velocities, respectively. The NO_X production at the representative inlet condition was still low as ~ 1EI. Decreasing pressure, increasing temperature, or decreasing velocity, however, increased the NO_X production. The increase was primarily due to higher specific plasma power deposition, more significant thermionic emission and elevated reduced electric field.

6. Acknowledgement

The material is based upon work supported by NASA under award No. NNX14AF53A with Dr. Koushik Datta as a technical officer. The PI would like to thank to Drs. Jordan Snyder, Jeffrey Cohen, Scott Liljenberg, Seung-Bum Kim, Paul Palies, Lance Smith, Adam Holley and Donald Hautman for their helpful comments. Also, we appreciate the efforts of Mr. John Costello and Mr. Jay Borst for the test and experiment setup.

7. Disclaimer

Any opinions, findings, and conclusions or recommendations expressed in this material are those of the authors and do not necessarily reflect the views of the National Aeronautics and Space Administration.

8. References

1. Y. Ju, W. Sun, Prog. In Ener. and Comb. Sci. 48 (2015) 21–83.

2. A. Bao, Y.G. Utkin, S. Keshav, G. Lou, I.V. Adamovich, IEEE Trans. Plasma Sci. 35 (6) (2007) 1628–1638.

3. C. D. Cathey, T. Tang, T. Shiraishi, T. Urushihara, A. Kuthi, M.A. Gundersen, IEEE Trans. Plasma Sci. 35 (6) (2007) 1664–1668.

4. W. Kim, H. Do, M. G. Mungal, M. A. Cappelli, IEEE Trans. Plasma Sci. 34 (6) (2006) 2545-2551.

5. H. Do, S. Im, M. A. Cappelli, M. G. Mungal, Combust. Flame 157 (2010) 2298–2305.

6. D. A. Lacoste, J. P. Moeck, D. Durox, C. O. Laux, T. Schuller, J. Eng. Gas Turbines Power 135 (10) (2013) 101501 (7 pages).

7. D. Gysling, G. Copeland, D. McCormick, W. Proscia, J. Eng. Gas Turbines Power 122 (2) (1999) 269–274.

8. F. E. C. Culick, V. Yang, Overview of Combustion Instabilities in Liquid-Propellant Rocket Engines. In: Liquid Rocket Engine Combustion Instability. Progress in Astronautics and Aeronautics, American Institute of Aeronautics and Astrophysics, Washington, DC, 1995, p. 3.

9. R. P. Pandalai, H. C. Mongia, Combustion instability characteristics of industrial engine dry low emission combustion systems, 34th AIAA/ASME/SAE/ASEE Joint Propulsion Conference and Exhibit, Cleveland, OH, 1998.

10. W. Polifke, J. Kopitz, A. Serbanovic, Impact of the Fuel Time Lag Distribution in Elliptical Premix Nozzles on Combustion Stability, 7th AIAA/CEAS Aeroacoustics Conference, Maastrich, NL, 2001.

11. J. M. Cohen, A. Banaszuk, J. Prop and Power 19 (5) (2003) 811–821.

12. T. Lieuwen, V. Yang, Eds., Combustion Instabilities in Gas Turbine Engines: Operational Experience, Fundamental Mechanisms, and Modeling, AIAA Progress in Aeronautics and Astronautics Series, 210, 2005, p. 657.

13. W. Kim, H. Do, M. G. Mungal, M. A. Cappelli, IEEE Trans. Plasma Sci. 36 (6) (2008) 2898-2904.

14. T. Lieuwen, Unsteady Combustor Physics, Cambridge University Press, Cambridge, U.K., 2012, pp. 103-107.

15. I. Chterev, C.W. Foley, S. Kostka, A.W. Caswell, N. Jiang, J.M. Seitzman, T.C. Lieuwen, Flame and flow topologies in an annular swirling flow, Proceedings of ASME Turbo Expo, San Antonio, Texas, 2013.

16. D. Burnette, I. Shkurenkov, I. V. Adamovich, W. R. Lempert, Kinetics of NO formation and decay in nanosecond pulse discharges in air-fuel mixtures, 53rd AIAA Aerospace Science Meeting, Kissimmee, FL, 2015.

17. N. A. Popov, Plasma Physics Reports 27 (2001) 886.